White lines in the $L_{2,3}$ electron-energy-loss and x-ray absorption spectra of $3d$ transition metals

W. G. Waddington*
Department of Metallurgy and Science of Materials, University of Oxford, Parks Road, Oxford OX1 3PH England

P. Rez†
Center for Solid State Science and Department of Physics, Arizona State University, Tempe, Arizona 85287

I. P. Grant
Department of Theoretical Chemistry, University of Oxford, South Parks Road, Oxford OX1 3PH England

C. J. Humphreys‡
Department of Metallurgy and Science of Materials, University of Oxford, Parks Road, Oxford OX1 3PH England
(Received 28 January 1986)

In the electron-energy-loss or x-ray-absorption spectra of the $3d$ transition metals the onset of the $L_{2,3}$ edge ($2p$ excitation) is marked by two sharp peaks often called white lines. The peaks are attributed to the excitation of the $2p_{3/2}$ and $2p_{1/2}$ subshells to unoccupied d levels but the observed ratio of their areas is not the statistical 2:1 ratio expected from initial-state occupation. In this paper we report the results of multiconfiguration Dirac-Fock calculations of the transition rates which should include atomic many-electron effects. We compare our results with experimental energy-loss measurements from a number of sources. There is good agreement for the ratio of the two components although the detailed shape can show additional solid-state effects. In particular, the L_3-L_2 ratio is very sensitive to the charge state for elements in the middle of the period such as Mn and Cr. This effect can therefore be used to measure ionicity in energy-loss microanalysis in the electron microscope.

INTRODUCTION

Sharp peaks at the thresholds of absorption edges were first observed by x-ray absorption for the L edges of heavy elements such as Pt. As early observations were made photographically, the peaks were seen as white lines on the photographic plate. The name has remained even though photographic recording has been superceded by electronic data-acquisition systems (see Refs. 1 and 2 for general review of white-line observations). White lines in the $2p$ spectra from the transition metals were first observed by Cauchois and Bonnelle[3,4] by x-ray absorption. For small scattering angles the energy-loss spectrum of high-energy ($\sim$100 kV) electrons transmitted through thin specimens in an electron microscope is identical to the x-ray-absorption spectrum. The energy-loss experiments of Leapman and Grunes[5,6] showed that the ratio of the two spin-orbit components from the $2p_{3/2}$ and $2p_{1/2}$ transitions did not follow the statistical 2:1 ratio expected from the ratio for the initial states. Various nonrelativistic band calculations failed to reproduce the observed effect and other "many-electron" explanations were proposed. The electron-energy-loss results were confirmed by synchrotron-radiation x-ray-absorption studies for calcium, scandium, and titanium by Barth *et al.*,[7] who believed that the results could be explained using an atomic theory without solid-state effects. There have been other synchrotron results for calcium[8] and copper in copper oxide.[9] Similar white-line effects have been observed in the $3d$ absorption spectra of rare-earth elements, initially by x-ray-absorption spectroscopy and later by electron-energy-loss spectroscopy (EELS). The ratios of the M_5 ($3d_{5/2}$) and M_4 ($3d_{3/2}$) spin-orbit components do not equal the initial-state 3:2 ratio. Atomic multiplet calculations, in which the transition rates are calculated by perturbation theory on a nonrelativistic Schrödinger equation[10–14] gave reasonable agreement with the white-line structure at the ends of the rare-earth-metal period. The most recent example of this approach is a full multiplet calculation for all the rare-earth elements.[15]

An alternative to the atomic multiplet approach has been the relativistic linear combination of atomic orbitals (LCAO) band calculation of Mattheis and Deitz.[16] They leave the number of holes in the two bands associated with the spin-orbit components as a parameter which can be determined by accurate band calculations or experiment. This has been used recently to explain magnetic ordering in amorphous metals.[17] Other recent experimental work has concentrated on energy-loss measurements of various $3d$ transition metals in different compounds showing different degrees of ionicity.[18]

In this paper we apply an atomic multiconfiguration Dirac-Fock (MCDF) program to the $2p$ excitation.[19] The program handles both electrostatic and spin-orbit effects automatically as part of the Dirac formalism. The more familiar atomic multiplet method of calculation—for example, in the work of Sugar[10]—treats the spin-orbit interaction as a perturbation of an essentially nonrelativistic problem. It is also customary in these calculations to scale down the electrostatic and exchange parameters by

20%.[15] Another advantage of our approach is that the program generates the configurations automatically from the subshell occupation numbers. This is convenient for elements in the middle of the period, where there are many possible arrangements, making it difficult to keep track of them without the computer.

THEORY

The atomic multiconfiguration Dirac-Fock program of Grant *et al.*[19] was used to calculate atomic-state wave functions, and a modified version of the transition-rate program used by Dyall and Grant[20] gave the line strengths. In this approach the Hamiltonian for the N-electron atom is given by

$$H=\sum_i [c\boldsymbol{\alpha}\cdot\mathbf{p}_i+(\beta-1)c^2-Z/r_i]+\sum_{\substack{i,j\\(i<j)}}^{N}\frac{1}{|\mathbf{r}_i-\mathbf{r}_j|}\ , \tag{1}$$

where $\boldsymbol{\alpha},\beta$ are the Dirac matrices, $\mathbf{p}_i$ is the momentum, and $\mathbf{r}_i$ the position of the ith electron, and atomic units have been used ($m=e=\hbar=1$). The wave functions are constructed from the central-field Dirac orbitals given by

$$U_{n\kappa m}(\mathbf{r})=\frac{1}{r}\begin{bmatrix} P_{n\kappa m}(r) & \chi_{\kappa,m}(\mathbf{r}) \\ iQ_{n\kappa m}(r) & \chi_{-\kappa,m}(\mathbf{r})\end{bmatrix}\ , \tag{2}$$

where

$$\chi_{\kappa,m}=\sum Y_{l,m-\sigma}(\mathbf{r})\phi^{\sigma}C(l,\tfrac{1}{2},j;m-\sigma,\sigma)$$

and κ is defined as $-2(j-l)(j+\frac{1}{2})$, j is the total angular-momentum quantum number $l+s$ ($\frac{1}{2}$, $\frac{3}{2}$, etc.), and l corresponds to the orbital angular momentum in an lsj coupling representation. The orbitals form an orthonormal set such that

$$\int (P_aP_b+Q_aQ_b)dr=\delta_{a,b}\ .$$

Configuration-state functions are defined as N-electron states of prescribed total angular-momentum quantum number J and parity, in which the N electrons present have prescribed assignments to the available subshells. They may be constructed, for example, as a linear combination of Slater determinants built from the orbitals $U_{n\kappa m}$. In practice, the code uses methods based on Racah angular-momentum algebra; j-j coupled states are defined for each subshell, giving a resultant angular momentum J_i, and these are then vector-coupled in the usual way to give the resultant J. Such configurational states $\phi(\gamma,J,M)$ are eigenstates of N uncoupled electrons, moving as described by Dirac's equation in a static central potential. The label carries information needed along with the angular-momentum quantum numbers to identify the configuration-state function (CSF) uniquely. The electrostatic interaction between the electrons mixes configurational states of the same angular symmetry; we denote the resultant linear combination as an atomic-state function,

$$\psi_{\alpha}(JM)=\sum_{r=1}^{n_c} c_r(\alpha)\phi(\gamma_r JM)\ , \tag{3}$$

where n_c is the number of configuration-state functions and $c_r(\alpha)$ are the configuration-mixing coefficients for atomic-state α. The energy of atomic state α is given by

$$E_{\alpha}=\int \psi^{\dagger}{}_{\alpha}(JM)H\psi_{\alpha}(JM)d\tau=\sum_{r,s} c_r^*(\alpha)H_{rs}c_s(\alpha)\ , \tag{4}$$

$$H_{rs}=\int \phi^{\dagger}(\gamma_r JM)H\phi(\gamma_s,J,M)d\tau\ . \tag{5}$$

The configuration-mixing coefficients can be determined from the requirement that E_{α} be stationary with small variations in the coefficient, and the normalization requirement $\langle U_{\alpha}\,|\,U_{\alpha}\rangle=1$, giving an eigenvalue equation

$$(H-E_{\alpha}I)\mathbf{c}_{\alpha}=0\ . \tag{6}$$

The wave functions are calculated for both the ground state and a final state in which there is a hole in the $2p$ subshells and an extra electron in the $3d$ subshell. The transition strengths are calculated according to a dipole selection rule and tabulated according to the energy of the transition. In these calculations a frozen core was used, so relaxation effects are not taken into account. The program does, however, allow for an arbitrary definition of the core state to be made; therefore relaxation effects could be investigated. Those many-electron effects resulting from different arrangements in the $3d$ subshells are included in these calculations. Because the d wave functions are relatively tightly bound and the d band is quite narrow, it is expected that an atomic theory can be justified in the study of these transitions.

CALCULATIONS AND COMPARISON WITH EXPERIMENT

The transition rates were calculated for various configurations corresponding to known charge states for the $3d$ transition-metal elements. For comparison with experiment these were convoluted with a Gaussian representing both instrumental broadening effects and finite lifetime of the core hole. The core-hole lifetimes were estimated from the radiationless and radiative transition rate of McGuire[21] and Walters and Bhalla.[22] For these low-energy transitions the most important physical line-broadening mechanism is radiationless Auger transitions, but the observed linewidth in energy-loss experiments is dominated by instrumental broadening, which is 1.5 eV for the data in Ref. 23. Estimates of the ratio between the two white-line components can be made by measuring the peak heights from the synthesized spectra. Measuring the change in the ratio of the areas can give different results in those cases where the two components have different calculated line shapes. It is then sometimes difficult to distinguish where one component ends and the other begins. The instrumental broadening does not have much effect on the calculated ratio.

Experimental spectra for transition-metal oxides were taken from the data of Ref. 23. Backgrounds were first subtracted by fitting the usual AE^{-r} function in the re-

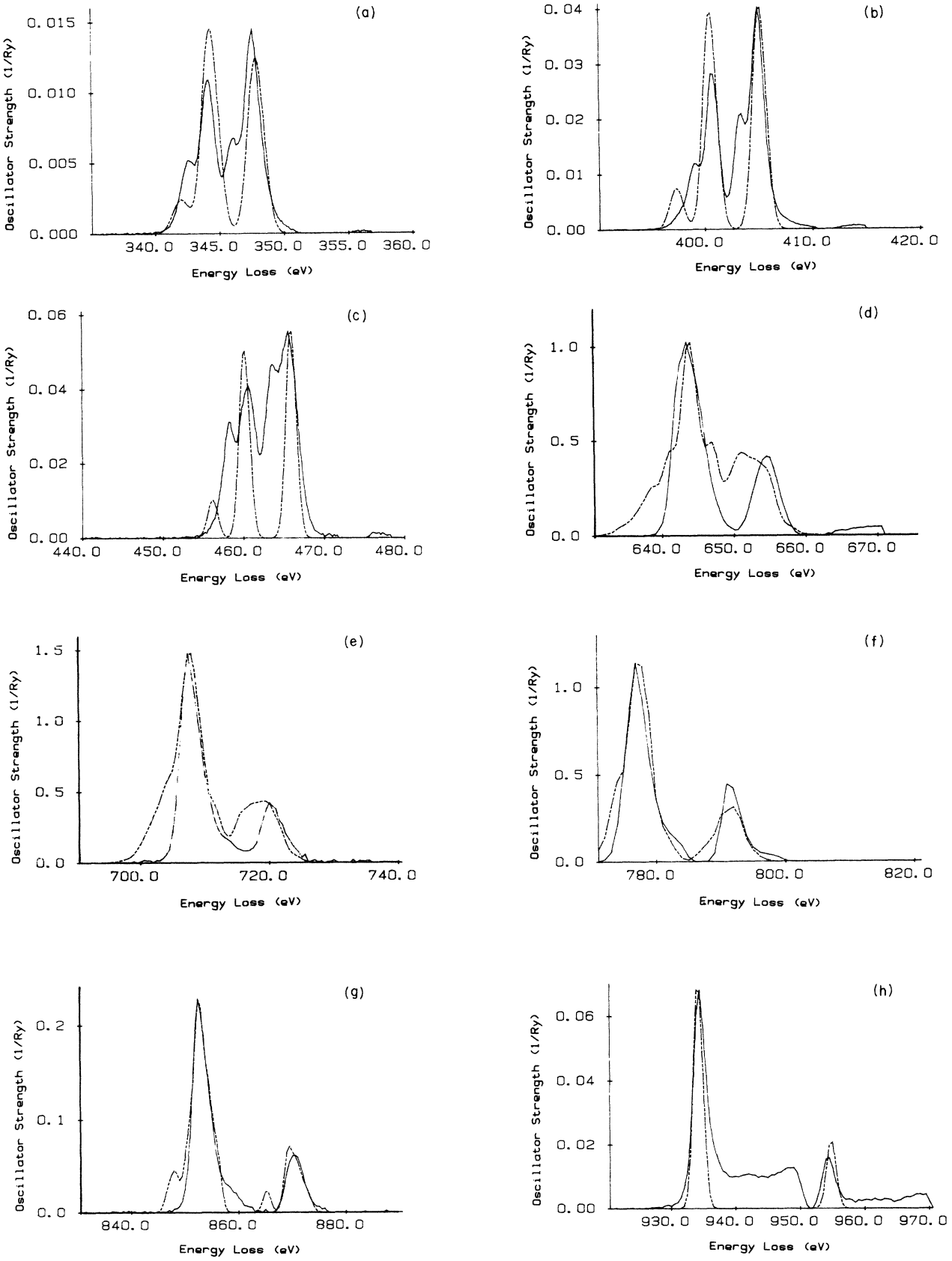

FIG. 1. Comparison of calculated spectral shape with EELS Atlas data. Solid lines, experimental spectra; dashed lines, calculated spectra. (a) Ca^{2+} in $CaCo_3$; (b) Sc^{3+} in Sc_2O_3; (c) Ti^{4+} in TiO_2; (d) Mn^{4+} in MnO_2; (e) Fe^{3+} in Fe_2O_3; (f) Co^{2+} in CoO; (g) Ni^{2+} in NiO; (h) Cu^{2+} in CuO.

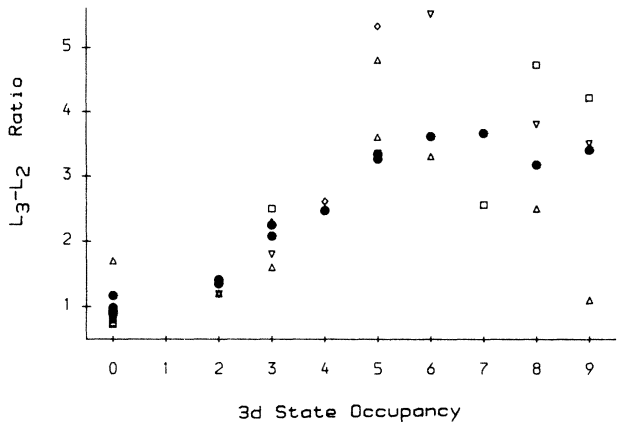

FIG. 2. Variation of white-line ratios with d-state occupation. ●, calculated results; △, Sparrow *et al.*, Ref. 18; ∇; Leapman *et al.*, Ref. 6; □, EELS Atlas, Ref. 22; ◇, Miner and Rask, Ref. 27.

gion before the edge, where E is the energy loss and A and r are constants. The transitions to continuum states then had to be subtracted from the spectra. This was done by fitting the results of continuum spectra calculations[24,25] to a region about 20—40 eV above the edge. The starting energy for the continuum contribution was to some extent arbitrary, but reasonable shifts resulted in differences of less than 5% of the ratio of the two components. This spectrum could then be compared with the theoretical MCDF spectra, and the results are given as Fig. 1. The ratio of the two white-line components could also be estimated from these experimental spectra. The main trend in both the experimental and calculated results is the change in the line ratio from about 0.6:1 for Sc^{3+} to 0.3:1 for Cu^{2+}. It appears that the line ratio is most strongly related to the d-state occupation number, which is also shown graphically as Fig. 2. The details of the calculated line shape do not fit the experimental line shapes for the first few elements, Ca^{2+}, Sc^{3+}, and Ti^{4+}. The splitting in the two spin-orbit components observed experimentally in these elements is due to transitions to molecular-orbital levels such as $2t_{2g},3e_g$ in TiO_2.[26] Obviously, to calculate the details of the white-line shape, solid-state effects have to be included in the theory. The agreement appears to be much better for elements such as Co^{2+} and Ni^{2+}. Although the ratios of the two white-line components are approximately correct for Mn^{4+} and Fe^{3+}, the details of the line shape are not calculated correctly, again probably due to neglect of solid-state effects. These could be incorporated by a LCAO treatment similar to that of Mattheis and Deitz.[16] The extra structure in the copper spectrum is due to problems with subtracting the continuum contribution.

Calculated white-line ratios for a number of different cation charge states are compared with various experimental results in Table I and Fig. 2. Not all the discrepancies are due to problems in the theoretical treatment. As can be seen, the differences between different experiments is sometimes greater than the difference between any of the experiments and these calculations. This is particularly true for elements towards the end of the

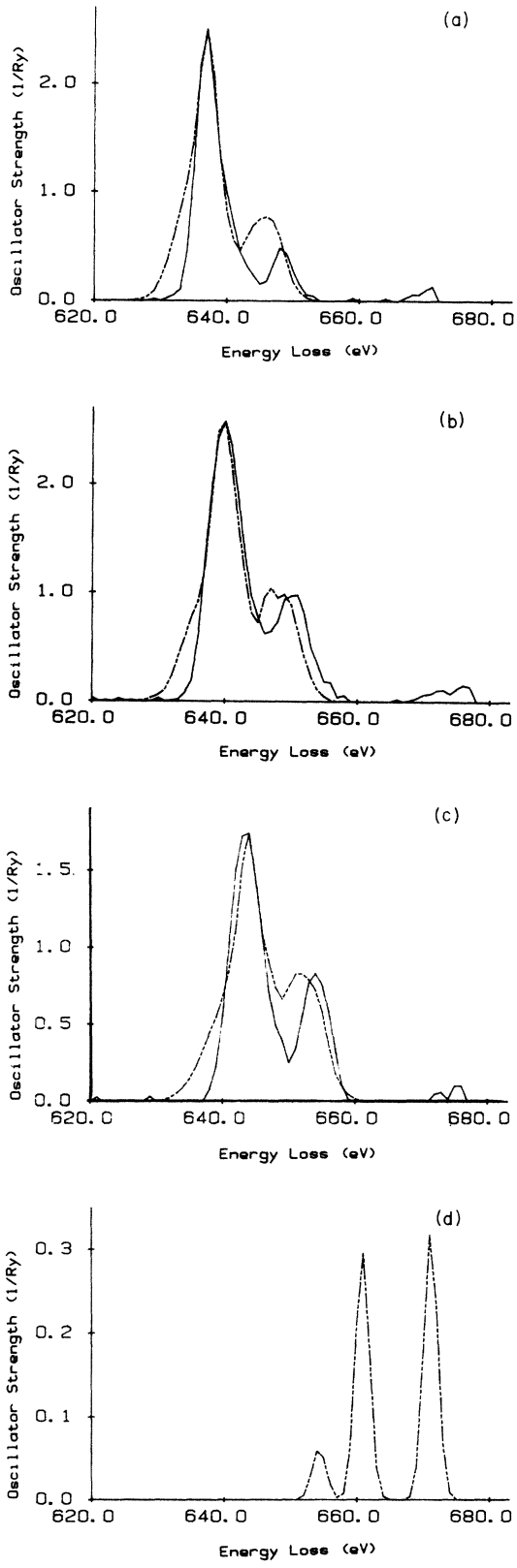

FIG. 3. Comparison of calculated spectra of manganese in various charge states with experimental data of Miner and Rask. Solid lines, experimental spectra; dashed lines, calculated spectra. (a) Mn^{2+} in MnO; (b) Mn^{3+} in Mn_2O_3; (c) Mn^{4+} in Mn_3O_4; (d) Mn^{7+}.

period where the L_2 line is much smaller than the L_3 line and experimental errors in the ratio measurement will be greater. It must be remembered that the spectra of Sparrow *et al.*,[18] Leapman *et al.*,[6] and Miner and Rask[27] were taken at lower resolution (of order 4 eV) than the spectra in Ref. 23. The procedure used to extract the white-line ratio also varied. Leapman *et al.*[6] used a deconvolution technique which can effectively remove the instrumental broadening. It makes the assumption that the L_3 and the L_2 components have the same shape and that the continuum contributions also follow the white-line ratios. There are problems with both these assumptions. From the spectra shown it is apparent that the L_3 and L_2 lines need not have the same shape. There is also no reason to believe that the continuum excitations do not follow the 2:1 ratio. The experimental fit for pure copper when the *d* states are filled shows a 2:1 ratio, as do fits to the continuum part of the Co^{2+} and Ni^{2+} spectra.

The ratio between the L_3 and L_2 lines can be quite sensitive to the electronic configuration and hence the charge state of the transition-metal cation. This is especially true for those elements towards the middle of the Periodic Table row such as Mn and Cr. The variation of the ratio should be distinguishable even for relatively low concentrations of the element in a microanalytic experiment. In Fig. 3 the calculated spectrum shape assuming 4 eV instrument resolution is compared with the experimental results of Miner and Rask[27] for manganese in MnO (Mn^{2+}), Mn_2O_3 (Mn^{3+}), and MnO_2 (Mn^{4+}). Also shown is the calculated spectrum for Mn^{7+}. Except in the case of MnO [Fig. 3(a)], the agreement is very good and it shows that it should be possible to use the results of such calculations to determine the cation charge. The degradation in instrument resolution has also eliminated the structure due to the different lines making up the white-line components [compare Fig. 1(d) with Fig. 3(c)]. Sparrow *et al.*[18] also measured the manganese $L_{2,3}$ edge in $KMnO_4$, which they believe represents the Mn^{7+} state. Not only is the white-line ratio in disagreement with the experiments, but the calculations also show a shift of the lines to higher energies. It is very doubtful that Mn in these experiments is in the Mn^{7+} state for very long. Po-

TABLE I. Calculated and measured L_3-L_2 ratios for transition-metal ions.

	Calc.	Expt.[a]	Expt.[b]	Expt.[c]	Expt.[d]
Ca	1.29				
Ca^+	1.24				
Ca^{2+}	1.17			0.75±0.03	
Sc	1.49				
Sc^+	1.49				
Sc^{2+}	1.37				
Sc^{3+}	0.97			0.73±0.03	
Ti	1.58				
Ti^+	1.59				
Ti^2	1.51				
Ti^{4+}	0.91		0.8	0.80±0.03	
V	2.12				
V^{3+}	1.46	1.2	1.19		
V^{5+}	0.89	1.0			
Cr^{3+}	2.08	1.6	1.8		
Cr^{4+}	1.37	1.4			
Mn^{2+}	3.25	4.8			5.32
Mn^{3+}	2.50				2.61
Mn^{4+}	2.25			2.50±0.03	2.09
Mn^{7+}	0.93				
Fe^{2+}	3.61		5.5		
Fe^{3+}	3.43			3.35±0.03	
Co^{2+}	3.67			2.56±0.2	
Ni^{2+}	3.22	2.5	3.8	4.72±0.2	
Cu^+	3.30				
Cu^{2+}	3.30	1.1	3.5	4.21±0.2	

[a]Reference 18, Sparrow *et al.*
[b]Reference 6, Leapman *et al.*
[c]Reference 23, EELS Atlas.
[d]Reference 27, Miner and Rask.

tassium is very volatile even under extremely low electron-beam doses and it is quite possible that the material is transformed to MnO_2 with the potassium and oxygen escaping. This could be investigated by experiments at low temperature and careful study of the potassium edge in the spectrum along with the diffraction pattern. The results of Sparrow *et al.*[18] also contradict other results for Cu^{2+}, where most of the experiments show an L_3-L_2 ratio much greater than 2:1. The other element which shows large variations with charge state is Cr. The plot of allowed transitions for Cr^{3+} and Cr^{4+} is given as Fig. 4 and synthesized spectra assuming 2 eV energy resolution are given as Fig. 5. The changes in white-line ratio as well as the difference in the number of transitions are apparent from the plots.

For simple cases where there are few transitions involved it is possible to identify the individual lines. For Ca^{2+}, Sc^{3+}, and Ti^{4+} the transition can be represented by a configuration $2p^6$ going to $2p^5 3d$. The lower-energy line has components from the $p_{3/2}$-to-$d_{3/2}$ and $p_{3/2}$-to-$d_{5/2}$ transitions, while the higher-energy line arises from $p_{1/2}$-to-$d_{3/2}$ transitions. For Cu^{2+} the transition is $2p^6 3d^9$ to $2p^5 3d^{10}$. The lower-energy line again corresponds to the $2p_{3/2}$-to-$3d_{3/2}$ and -$3d_{5/2}$ configurations, while the higher-energy line corresponds to the $2p_{1/2}$-to-$3d_{3/2}$ transition. In intermediate cases such as Mn and Fe it is not possible to rigidly separate each of the white lines into $2p_{3/2}$ and $2p_{1/2}$ components, though the lower-energy line mainly arises from $2p_{3/2}$ transitions and the higher-energy line from $2p_{1/2}$ transitions.

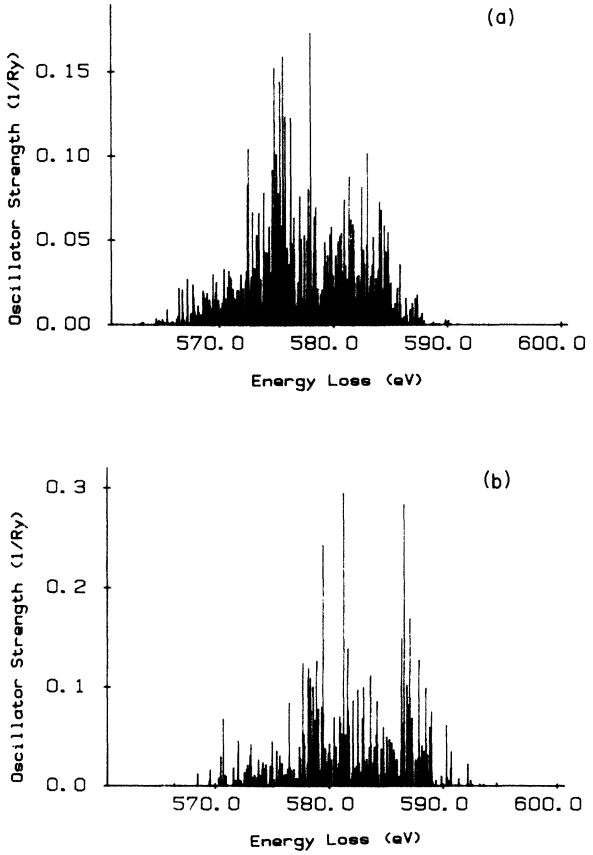

FIG. 4. Calculated transitions for Cr. (a) Cr^{3+}; (b) Cr^{4+}.

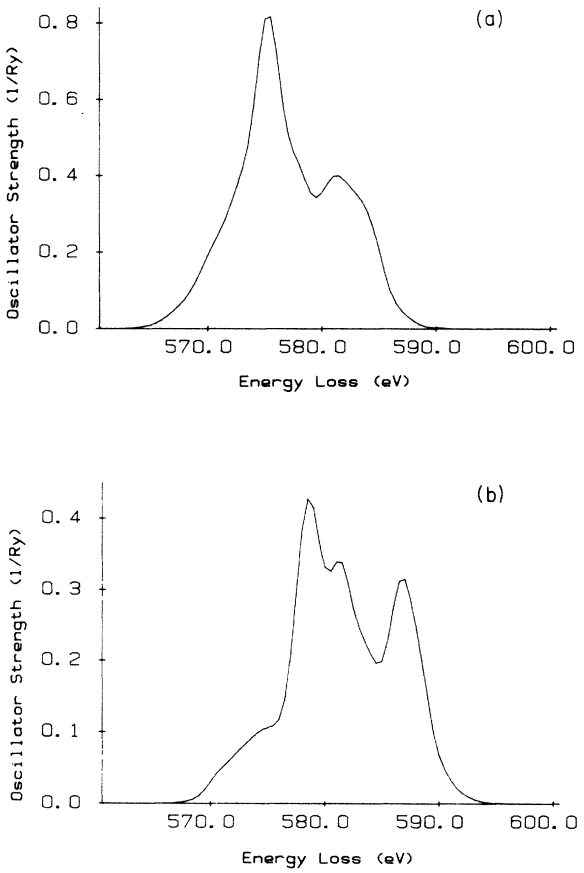

FIG. 5. Calculated spectra for Cr assuming 2 eV resolution. (a) Cr^{3+}; (b) Cr^{4+}.

CONCLUSIONS

Calculations using an atomic multiconfiguration Dirac-Fock theory account for the variations in the L_3-L_2 white-line ratio of the $3d$ transition metals. The details of the shapes of the white lines, especially for Ca^{2+}, Sc^{3+}, and Ti^{4+} in their respective oxides, are often dominated by molecular-orbital splitting. For elements such as Mn and Cr, the L_3:L_2 ratio is sensitive to electronic configuration or cation charge and can be used as a way of measuring charge state in microanalytical applications. The one electron view that the lower-energy line is entirely due to the $2p_{3/2}$ excitation and the higher-energy line is entirely due to the $2p_{1/2}$ excitation does not correctly describe all aspects of these transitions.

ACKNOWLEDGMENTS

We are grateful to Dr. C. Ahn and Dr. O. L. Krivanek for making available the EELS Atlas spectra of Ref. 23, and B. Miner and J. Rask for allowing us to use various manganese spectra. We should also like to thank Dr. G. Thornton for useful suggestions.

*Present address: Department of Earth Sciences, University of Oxford, Parks Road, Oxford OX1 3PR England.
†To whom correspondence should be addressed.
‡Present address: Department of Metallurgy and Materials Science, University of Liverpool, P.O. Box 147, Liverpool L69 3BX England.

[1]P. S. P. Wei and F. W. Lytle, Phys. Rev. B **19**, 679 (1979).
[2]M. Brown, R. E. Peierls, and E. A. Stern, Phys. Rev. B **15**, 738 (1972).
[3]Y. Cauchois and C. Bonnelle, C. R. Acad. Sci. Paris **245**, 1230 (1957).
[4]C. Bonnelle, C. R. Acad. Sci. Paris **248**, 2324 (1959).
[5]R. D. Leapman and L. A. Grunes, Phys. Rev. Lett. **45**, 397 (1980).
[6]R. D. Leapman, L. A. Grunes, and P. L. Fejes, Phys. Rev. B **26**, 614 (1982).
[7]J. Barth, F. Gerken, and C. Kunz, Phys. Rev. B **28**, 3608 (1983).
[8]M. W. D. Mansfield, Proc. R. Soc. London, Ser. A **348**, 143 (1976).
[9]S. L. Hulbert, B. A. Bunker, F. C. Brown, and P. Pianetta, Phys. Rev. B **30**, 2120 (1984).
[10]J. Sugar, Phys. Rev. A **6**, 1764 (1962).
[11]C. Bonnelle, R. C. Karnatak, and J. Sugar, Phys. Rev. A **9**, 1920 (1974).
[12]C. Bonnelle, R. C. Karnatak, and N. Spector, J. Phys. B **10**, 795 (1977).
[13]N. Spector, C. Bonnelle, G. Dufour, C. K. Jorgensen, and H. Berthou, Chem. Phys. Lett. **41**, 199 (1976).
[14]J. Sugar, W. D. Brewer, G. Kalkowski, G. Kaindl, and E. Paparazzo, Phys. Rev. B **32**, 2242 (1985).
[15]B. J. Thole, G. Van der Laan, J. C. Fuggle, G. A. Sawatzky, R. C. Karnatak, and J.-M. Esteva, Phys. Rev. B **32**, 5107 (1985).
[16]L. F. Mattheis and R. E. Deitz, Phys. Rev. B **22**, 1663 (1980).
[17]T. L. Morrison, M. B. Brodsky, J. R. Sill, and N. J. Zaluzec, Phys. Rev. B **23**, 3107 (1985).
[18]T. G. Sparrow, B. G. Williams, C. N. R. Rao, and J. M. Thomas, Chem. Phys. Lett. **108**, 547 (1984).
[19]I. P. Grant, B. J. McKenzie, P. M. Norrington, D. F. Mayers, and N. C. Pyper, Comput. Phys. Commun. **21**, 207 (1980).
[20]K. G. Dyall and I. P. Grant, J. Phys. B **17**, 1281 (1984).
[21]E. J. McGuire, Phys. Rev. A **3**, 587 (1971).
[22]D. L. Walters and C. P. Bhalla, Phys. Rev. A **4**, 2164 (1971).
[23]C. C. Ahn and O. L. Krivanek, EELS Atlas, report of the Arizona State University High Resolution Electron Microscopy Facility and Gatan, Inc. (890 Commonwealth Dr., Warrendale, PA 15086) (1982) (unpublished).
[24]R. D. Leapman, P. Rez, and D. F. Mayers, J. Chem. Phys. **72**, 1233 (1980).
[25]C. C. Ahn and P. Rez, Ultramicroscopy **17**, 105 (1985).
[26]L. A. Grunes, R. D. Leapman, C. N. Wilker, P. Hoffmann, and A. B. Kunz, Phys. Rev. B **25**, 7157 (1982).
[27]B. Miner and J. M. Rask (private communication).

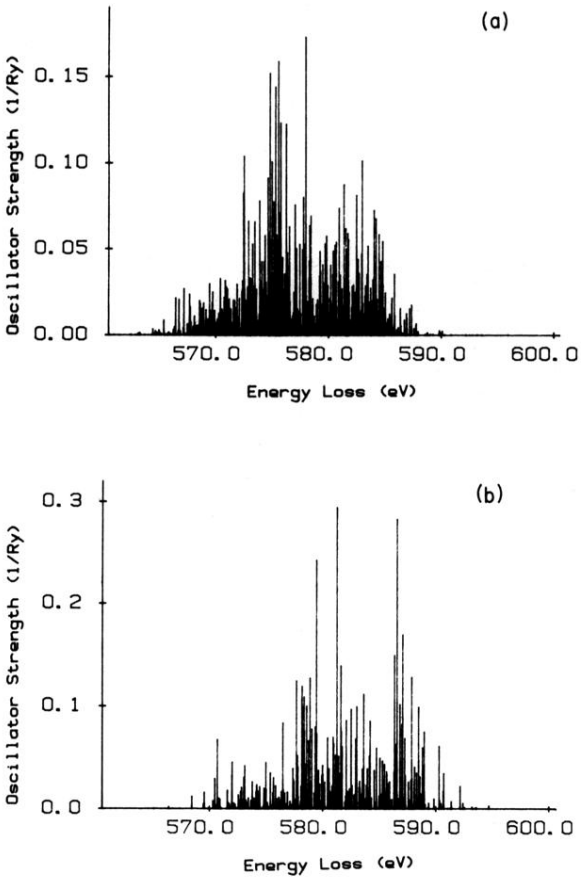

FIG. 4. Calculated transitions for Cr. (a) Cr^{3+}; (b) Cr^{4+}.